THE JOURNAL OF BIOLOGICAL CHEMISTRY VOL. 288, NO. 9, pp. 6295–6305, March 1, 2013

Chaperone Stress 70 Protein (STCH) Binds and Regulates Two Acid/Base Transporters NBCe1-B and NHE1*

Received for publication, June 15, 2012, and in revised form, January 8, 2013 Published, JBC Papers in Press, January 9, 2013, DOI 10.1074/jbc.M112.392001

Jun-Seok Bae[‡], Na-Youn Koo[‡], Eun Namkoong[‡], Alexander J. Davies[‡], Seul-Ki Choi[‡], Yonghwan Shin[‡], Meihong Jin[‡], Sung-Min Hwang[‡], Katsuhiko Mikoshiba[§], and Kyungpyo Park[‡1]

From the [‡]Department of Physiology, School of Dentistry, Seoul National University and Dental Research Institute, Seoul 110-749, Republic of Korea and the [§]Laboratory for Developmental Neurobiology, RIKEN Brain Science Institute, Wako, Saitama 351-0198, Japan

Background: Regulation of intracellular pH is critical for cellular homeostasis.
Results: Stress 70 protein chaperone (STCH) interacts with pH regulating transporters NBCe1-B and NHE1 and modulates their functional expression.
Conclusion: STCH chaperone dynamically regulates intracellular pH through site-specific interactions with ion transporters.
Significance: These novel STCH interactions provide a mechanism for intracellular pH regulation in response to homeostatic stress.

Regulation of intracellular pH is critical for the maintenance of cell homeostasis in response to stress. We used yeast two-hybrid screening to identify novel interacting partners of the pH-regulating transporter NBCe1-B. We identified Hsp70-like stress 70 protein chaperone (STCH) as interacting with NBCe1-B at the N-terminal (amino acids 96–440) region. Co-injection of STCH and NBCe1-B cRNA into *Xenopus* oocytes significantly increased surface expression of NBCe1-B and enhanced bicarbonate conductance compared with NBCe1-B cRNA alone. STCH siRNA decreased the rate of Na^+-dependent pH_i recovery from NH_4^+ pulse-induced acidification in an HSG (human submandibular gland ductal) cell line. We observed that in addition to NBCe1-B, Na^+/H^+ exchanger (NHE)-dependent pH_i recovery was also impaired by STCH siRNA and further confirmed the interaction of STCH with NHE1 but not plasma membrane Ca^{2+} ATPase. Both NBCe1-B and NHE1 interactions were dependent on a specific 45-amino acid region of STCH. In conclusion, we identify a novel role of STCH in the regulation of pH_i through site-specific interactions with NBCe1-B and NHE1 and subsequent modulation of membrane transporter expression. We propose STCH may play a role in pH_i regulation at times of cellular stress by enhancing the recovery from intracellular acidification.

Regulation of intracellular pH (pH_i) is critical for myriad functions within the cell, and imbalance of pH_i can have severe consequences for cell survival. The electrogenic Na^+/HCO_3^- co-transporter (NBCe1)[2] is widely distributed and is essential for pH_i regulation (1). The intracellular level of HCO_3^- is also critical for fluid secretion by epithelial cells (2). The pancreatic isoform NBCe1-B (formerly pNBC1) is highly expressed in parotid and submandibular gland tissues in human (1), mouse (3), and guinea pig (4), which together share 95% sequence homology (4). The Na^+/H^+ exchangers (NHEs)[2] are another ion transporter family critical for pH_i regulation in epithelial cells (5). NHEs have also been implicated in cell growth and differentiation as well as a host of physiological functions in humans (6). Changes to pH_i due to NHE1 activity specifically were shown to regulate the timing of G_2/M entry and transition (7) as well as stimulate cell growth and proliferation (8).

The inositol 1,4,5-triphosphate receptor-binding protein, IRBIT, is the most well known mechanism of NBCe1-B regulation (9, 10). IRBIT enhances the activity of NBCe1-B via two distinct mechanisms; that is, directly by increasing the per-molecule activity of NBCe1-B (9, 11) and indirectly by antagonism of the with no lysine/SPAK (Ste20-related proline/alanine-rich kinase) kinase pathway, which normally functions to reduce the expression of NBCe1-B at the plasma membrane (10). IRBIT is also known to bind NHE3 and increase its activity in a Ca^{2+}-dependent manner (12). On the other hand a plethora of interacting partners have been reported for the ubiquitously expressed NHE1 that act to either directly regulate exchanger activity or as a scaffold for downstream signaling events (13). For example, calcineurin homologous protein 1 (CHP1) has recently been proposed to bind to NHE1 and enhance surface expression by stabilization at the plasma membrane (14). Despite these advances, data on NBCe1-B and NHE1 expression-modifying binding partners, especially in endogenous expression systems, remains scarce.

* This work was supported by a National Research Foundation of Korea grant through the Oromaxillofacial Dysfunction Research Center for the Elderly (2011-0028231) at Seoul National University in Korea.
[1] To whom correspondence should be addressed: Dept. of Oral Physiology, School of Dentistry, Seoul National University, Yeongeon Dong 28, Chongno Ku, Seoul 110-749, Republic of Korea. Tel.: 822-740-8658; Fax: 822-762–5107; E-mail: kppark@snu.ac.kr.
[2] The abbreviations used are: NBCe1, electrogenic Na^+/HCO_3^- co-transporter 1; NHE, Na^+/H^+ exchanger; BCECF/AM, 2′,7′-bis-(2-carboxyethyl)-5-(and-6)-carboxyfluorescein acetoxylmethyl ester; Bip, mammalian immunoglobulin-binding protein; DIDS, 4,4′-di-isothiocyano-2,2′-stilbenedisulfonic acid; EIPA, *S*-(*N*-ethyl-*N*-isopropyl) amiloride; hSMG, human submandibular gland; HSG cells, human submandibular gland ductal cell line; Hsp70, 70-kDa heat shock proteins; IRBIT, inositol 1,4,5-triphosphate receptor-binding protein; pH_i, intracellular pH; PMCA, plasma membrane Ca^{2+} ATPase; STCH, stress 70 protein chaperone; X-α-gal, 5-bromo-4-chloro-3-indolyl-α-D-galactopyranoside; ER, endoplasmic reticulum; μS, microsiemens; Hip, Hsp70 interacting protein; aa, amino acids.

Using yeast two hybrid screening we identified an interaction between NBCe1-B and the stress 70 protein chaperone STCH, a microsome-associated member of the 70-kDa heat shock protein (Hsp70) family that also encodes a core ATPase. Synonyms for STCH include "microsomal stress 70 protein ATPase core" and "heat shock 70-kDa protein member 13" (HSPA13). In humans STCH is constitutively expressed in all cell types and is induced by increases in cytoplasmic calcium but not by heat shock (15). Recent genomic studies have linked the *Stch* gene to several brain diseases such as Alzheimer disease, epilepsy, and autism (16–18). *Stch* has also been suggested as a candidate plasticity gene (19), and genetic mutations of *Stch* are thought to be associated with cancer occurring through tumor necrosis factor-related apoptosis-inducing ligand (TRAIL)-mediated apoptosis pathway (20). At the molecular level it is reported that STCH interacts with the ubiquitin-like proteins Chap1 and Chap2 (cyclic hydroxamic acid-containing peptide 1 and 2), which are known to modulate transit through the G_2/M phase of the cell cycle (21). However, the major cellular role of STCH has until now remained poorly understood.

In our study STCH increased the surface expression of NBCe1-B in transiently transfected *Xenopus* oocytes, and functional analysis showed that endogenous STCH was required for full recovery of NBCe1-B and NHE1 from acidic pH_i in human submandibular gland (HSG) ductal cells. Thus we demonstrate for the first time a role for STCH in pH_i regulation though the enhancement of NBCe1-B and NHE1 activity.

EXPERIMENTAL PROCEDURES

Yeast Two-hybrid Screening—Bait fragments (aa 96–440 of NBCe1-B) were cloned into the yeast binding domain vector pGBKT7 that carries the *trp1* gene (Clontech, Palo Alto, CA). For preparing prey construct, a library of human submandibular gland (hSMG) PCR products was prepared from poly(A)+ RNA according to manufacturer's protocols (Clontech). The hSMG PCR products linearized activation domain vector pGADT7-Rec (carrying the *leu2* gene). The bait construct and prey library were cotransformed into competent yeast cells (strain AH109) containing the MEL1 expression system that encodes α-galactosidase. Interaction of GAL4 (binding domain) and GAL4 (activation domain) fusion proteins enables the cells to grow on selection medium (−Ade/−Trp/−Leu/−His). Cotransformed yeast was cultured on a selection plate containing X-α-gal. Candidates were selected based on visualization of the blue α-galactosidase product.

Liquid α-Galactosidase Assay—Putative positive interactions between bait and prey proteins were analyzed using an α-galactosidase assay, which measures the quantity of enzyme secreted into the culture medium. Quadruple dropout liquid medium (lacking X-α-gal) was inoculated with positive colonies and incubated at 30 °C with shaking (250 rpm) until the absorbance at 600 nm reached 0.5–1.0 (16~18 h). Yeast cultures (1 ml) were centrifuged at 14,000 rpm for 2 min, and 8 μl of the supernatant was mixed with 24 μl of assay buffer. The reaction was incubated at 30 °C for 1 h and terminated by the addition of 960 μl of 0.1 M Na_2CO_3. The absorbance at 410 nm was measured, and α-galactosidase units were determined and compared with positive and negative controls.

Plasmids Construction—NBCe1-B wild type and N-terminal deletion mutants, aa 1–95 (Δ95aa) and 1–345 (Δ345aa), were cloned in pFLAG CMV2 vector and pBluescript II SK(+) vector to generate pFLAG CMV2-NBCe1-B, Δ95aa, and Δ345aa for expressing in HSG cells and pBluescript II SK(+)-NBCe1-B, Δ95aa, and Δ345aa for expressing in *Xenopus* oocytes, respectively. Also, STCH wild type and N-terminal deletion mutants aa 1–314 (Δ314aa) and 1–359 (Δ359aa) were cloned in pEGFP C1 vector and pBluescript II SK(+) vector to generate GFP-STCH, Δ314aa and Δ359aa for expressing in HSG cells and pBluescript II SK(+)-STCH, and Δ314aa and Δ359aa for expressing in *Xenopus* oocytes. NHE1 were cloned in pcDNA3.1(+) vector to generate pcDNA3.1(+)-NHE1 for expressing in HSG cells. All constructs were prepared from PCR product of HSG cells. The IRBIT construct was a gift from Katsuhiko Mikoshiba. All plasmids were confirmed by DNA sequencing.

Source of Human Submandibular Gland Tissue—hSMG tissue was acquired from patients who had submandibular glands resected as a treatment for a range of oral tumors. The group contained both men and women with ages ranging between 55 and 61 years. All patients gave informed consent for participation in this research. After surgical excision, the glands were instantly placed in cold (4 °C) physiological saline and transported to the laboratory for the experiments. The present study was allowed by the Institutional Review Board of Seoul National University Dental Hospital (CRI06002).

Reverse Transcription-Polymerase Chain Reaction—Total RNA was extracted from hSMG tissues and HSG cell lines using a TRI REAGENT (Sigma) following the manufacturer's instructions. The obtained RNAs were subjected to reverse transcription-polymerase chain reaction (RT-PCR) using oligo(dT) reverse transcriptase primers and Moloney murine leukemia virus reverse transcriptase (Invitrogen). The human GAPDH was amplified to assess the cDNA yield. Cycling parameters were as follows: 38 cycles of 94 °C for 45 s, 58 °C for 45 s, and 72 °C for 45 s.

Transfection and Co-immunoprecipitation—Transfection of HSG cells was performed by using Genefectine™ Reagent (Gentrone Biotech). HSG cells transfected constructs and hSMG tissues were lysed by lysis buffer containing 50 mM Tris-HCl, pH 8.0, 120 mM NaCl, 0.5% Nonidet P-40, 1 mM EDTA, *Xpert* protease inhibitor mixture solution (GenDEPOT, Barker, TX), 0.2 mM Na_3VO_4, 100 mM NaF for 15 min on ice and ultrasonicated 5 times for 10 s each. The lysates were centrifuged at 13,000 rpm for 20 min. The supernatants were precleaned by incubation with Protein A/G plus-agarose bead (Santa Cruz Biotechnology, Santa Cruz, CA) and incubated with antibody coupled to beads overnight. Immunoprecipitates were washed five times with same lysis buffer and subjected to Western blotting.

Where necessary, background contamination of heavy chain IgG in immunoprecipitation blots was removed with ReliaBLOT reagent (Bethyl Laboratories, Montgomery, TX) according to the manufacturer's instructions. Briefly, after Western blotting transfer, nitrocellulose membrane was blocked in 20 ml of ReliaBLOT block solution followed by incubated with primary antibody diluted in 15 ml ReliaBLOT block

solution overnight. Membranes were then washed three times in TBS-Tween buffer. ReliaBLOT HRP conjugate (anti-rabbit secondary antibody) was diluted in ReliaBLOT block solution at 1:5000 ratio. Membranes were again washed three times in TBS-Tween buffer, and the blot was developed as usual.

Immunofluorescence—Confluent HSG cells grown on coverglass bottom dishes were fixed with methanol for 5 min at −4 °C, rinsed with PBS, and permeabilized with 0.1% Triton X-100 for 10 min at room temperature. Then they were incubated for 1 h at room temperature in blocking solution, normal donkey serum (Jackson ImmunoResearch, West Grove, PA). Rabbit anti-STCH polyclonal antibody (Sigma) followed by Alexa Fluor® 488 goat anti-rabbit IgG (Invitrogen) was used to visualize endogenous STCH in HSG cells. A mouse monoclonal antibody against PDI (Abcam, Cambridge, CB4 0FL, UK) followed by Alexa Fluor® 594 donkey anti-mouse IgG (Invitrogen) was used for the detection of endoplasmic reticulum (ER). Slides were mounted with Vectashield mounting medium (Vector Laboratories, Burlingame, CA). Immunofluorescence images were acquired at ×100 magnification with a 1.40 N.A oil immersion lenses (Plan-Apochromat, DIC M27) using a confocal microscope (LSM 700, Carl Zeiss, Japan). All images were acquired with the same settings (ZEN2010 software, Zeiss). Fluorescence probes were excited and imaged sequentially, and colocalization was confirmed overlaying of the images. Images are representative of four independent experiments.

Synthesis of cRNAs—Capped RNAs were generated using a mMESSAGE mMACHINE® kit (Ambion, Austin, TX) according to the manufacturer's instructions. Briefly, plasmids containing NBCe1-B or STCH clones/pBluescript II SK(+) vector (Stratagene, La Jolla, CA) and IRBIT clones/PHM6 vector were linearized by a restriction enzyme digest, and cRNAs were obtained via an *in vitro* transcription reaction of the digestion products. For the reaction, 1 μg of purified linear template was mixed with transcription buffer, NTP/CAP, and T7 polymerase and incubated at 37 °C for 2 h. The template was removed by adding TURBO DNase to the reaction, and cRNAs were subsequently purified with a phenol-chloroform extraction and ethanol precipitation. The size, quantity, and quality of the *in vitro* transcription products were evaluated with denaturing agarose gel electrophoresis; cRNAs were stored in RNase-free water at −80 °C.

Electrophysiological Studies Using Xenopus laevis Oocytes—Oocyte were injected with NBCe1-B cRNA (5 ng) or coinjected with STCH cRNA (1 ng) with WPI Nanofilter 2000 via a sterile glass pipette and incubated at 18 °C for 2 days. NBCe1-B-mediated currents were measured in a HCO_3^--buffered solution containing 33 mM $NaHCO_3$, 66 mM NaCl, 2.0 mM KCl, 1.0 mM $MgCl_2$, 1.8 mM $CaCl_2$, 5 mM HEPES at pH 7.5 when bubbled with 5% CO_2. The current-voltage (*I-V*) relationship was determined by applying step voltage pulses from −160 to +60 mV from a holding potential of −25 mV. NBCe1 currents recorded in oocytes co-expressed with STCH and/or IRBIT were evoked by a single depolarizing step pulse from −120 to +20 mV. For membrane potential recordings, oocytes were first perfused with a HEPES-buffered solution 96 mM NaCl, 2.0 mM KCl, 1.8 v$CaCl_2$, and 5 mM HEPES, pH 7.5. Transporter activity was induced by changing to the HCO_3^--buffered solution. For Na^+-free solution, NaCl and $NaHCO_3$ were replaced by equimolar *N*-methyl-D-glucamine·Cl and choline-HCO_3^-, respectively.

Oocyte Immunoblotting and Immunofluorescence—Oocytes were injected with cRNA for NBCe1-B (5 ng) and STCH (1 ng). 48 h after injection, oocytes (30 per group) were homogenized in equal volume of buffer (0.3 M sucrose, 10 mM sodium phosphate, pH 7.4, *Xpert* protease inhibitor mixture solution (100×)). The homogenate was centrifuged at 3000 × *g* at 4 °C, and the supernatants were further centrifuged at 48,000 × *g* at 4 °C. Both the pellets (membrane fractions) were subjected to SDS/PAGE and immunoblotting. For visualizing NBCe1-B, oocytes were fixed overnight at 4 °C with 4% paraformaldehyde in PBS. After washing with PBS (3 × 5 min), oocytes were embedded in low melting point 3% agarose in PBS, and 20 μm sections were cut using a Cryocut Microtome (CM3050S, Leica). Sections were placed onto slides, blocked by incubation with normal donkey serum for 1 h at room temperature, and then incubated with rabbit anti-NBCe1 polyclonal antibody (Millipore) overnight at 4 °C. After washing again with PBS (3 × 5 min), oocytes were incubated with Alexa Fluor® 568 donkey anti-rabbit IgG (Invitrogen) for 1 h at room temperature. Sections were mounted with Vectashield mounting medium. Immunofluorescence images were acquired at ×10 magnification with a 0.3 N.A. lenses (Plan-Neofluar, Zeiss) using a confocal microscope (LSM 5 Pascal, Carl Zeiss, Japan). All images were acquired with the same settings. Membrane fluorescence intensity was analyzed in scaled image images (1 pixel = 2.5 μm) using the Plot Profile function within ImageJ (National Institutes of Health, Bethesda, MD).

Treatment with siRNA—After starvation for 3 h, HSG cells were transfected with 50 pmol of siRNA diluted in 250 μl of Dulbecco's modified Eagle's medium, and 10 μl of Genefectine was diluted in 250 μl of the same medium. The diluted siRNA and Genefectine were mixed and after 15 min were added to the dish. The final siRNA concentration was 10 nM. After 24 h, the medium was replaced with fresh DMED with serum.

pH_i Measurements—HSG cells were loaded with 2 μM BCECF-AM for 30 min at room temperature and washed twice with PBS buffer. pH_i recordings of HSG cells were obtained by measuring the fluorescence ratio using the MetaFluor® imaging system with fluorescence ratio imaging software (Version 7.6.5.0). BCECF-AM fluorescence was recorded at excitation wavelengths of 440 and 495 nm with an emission wavelength of 530 nm. Cells were perfused with either HCO_3^--buffered solution in 10 mM D-glucose, 10 mM HEPES, 115 mM NaCl, 5 mM KCl, 1 mM $MgCl_2$, 1 mM $CaCl_2$, 25 mM $NaHCO_3$, pH 7.5, or HEPES-buffered solution 10 mM D-Glucose, 10 mM HEPES, 140 mM NaCl, 5 mM KCl, 1 mM $MgCl_2$, 1 mM $CaCl_2$, pH 7.5. Intracellular acidification was induced by exposure to 20 mM NH_4Cl for 1 min in Na^+-free bath solution. For Na^+ free solutions, NaCl and/or $NaHCO_3$ were replaced by equimolar *N*-methyl-D-glucamine·Cl and choline-HCO_3^-, respectively. *S*-(*N*-Ethyl-n-isopropyl) amiloride (EIPA; 25 μm) and 4,4′-diisothiocyano-2,2′-stilbenedisulfonic acid (DIDS; 500 μm) were applied by adding to the bath solution at the final concentration. Bath solution was perfused at a flow rate of 3 ml/min. The resting pH_i of cells was calibrated using the high potassium nigericin procedure. Cells were perfused with five individual calibration

solutions 10 mM NaCl, 130 mM KCl, 0.8 mM $MgCl_2$, 20 mM HEPES, and 0.005 mM nigericin, pH 6.2, 6.6, 7.0, 7.4, 7.8.

Reagents—2′,7′-bis-(2-carboxyethyl)-5-(and-6)-carboxyfluorescein acetoxylmethyl ester (BCECF/AM) was obtained from Molecular Probes (Eugene, OR) and DIDS and EIPA were obtained from Sigma.

Surface Biotinylation—HSG cells were rinsed twice in PBS and incubated for 30 min at 4 °C with 0.5 mg/ml Sulfo-NHS-SS-Biotin (Pierce) in PBS. Cells were scraped, lysed, and sonicated 5 times for 1 s. The lysate was incubated on ice for 30 min with vortexing every 5 min for 5 s. Cell lysate was centrifuged at 10,000 × *g* for 2 min at 4 °C. Protein concentration was determined, and 1 mg of lysate was then incubated with NeutrAvidin-agarose (Pierce) for 1 h at room temperature. The agarose beads were washed in 3 times in wash buffer (Pierce). Biotinylated surface proteins were eluted by heating the beads at 80 °C for 10 min and then analyzed by Western blot. Bands were quantified by densitometry using the ImageJ program (National Institutes of Health). Densitometry values for surface protein expression were normalized to 100% of control biotinylated NHE1, plasma membrane Ca^{2+} ATPase (PMCA), and NBCe1-B.

Statistical Analysis—Data are presented as the mean ± S.E.; *n* is number of experimental repeats unless otherwise indicated. Statistical significances were assessed by analysis of variance; $p < 0.05$ was considered significant.

RESULTS

Identification of STCH as an NBCe1-B-binding Protein—We performed yeast two-hybrid screening of a hSMG prey cDNA library using a bait sequence encoding the intracellular N-terminal domain of NBCe1-B comprising 345 residues (aa 96–440) (Fig. 1*A*). Using a highly selective medium, 30 positive colonies were identified and isolated (Table 1). Plasmid DNA was selected from blue colonies exhibiting α-galactosidase activity and sequenced. Seven of 30 sequences contained open reading frame proteins found in the GenBank™ database. Of those seven sequences, STCH was identified in five colonies (Table 2). The strength of the NBCe1-B (bait) and STCH (target) interaction relative to controls was confirmed using an α-galactosidase assay (Fig. 1*B*). NBCe1-B and STCH mRNA transcripts were detected by RT-PCR in hSMG duct tissues, but not acinar tissues, isolated directly from human patients (Fig. 1*C*). We confirmed the interaction between endogenous STCH and NBCe1-B by performing a co-immunoprecipitation experiment in hSMG tissues (Fig. 1*D*).

Next, we examined the effect of STCH on the activity of NBCe1-B by performing two electrode voltage-clamp recordings in *Xenopus* oocytes. Oocytes were injected with NBCe1-B cRNA alone or co-injected with STCH cRNA. Oocytes were perfused with a HCO_3^--buffered solution bubbled with 5% CO_2, and the current generated from NBCe1-B was recorded as negative charge influx during step voltage pulses. Transporter conductance was determined from the current-voltage (*I-V*) relationship. Co-expression with STCH produced an ~2-fold increase in conductance (2.4 ± 0.1 μS) compared with NBCe1-B alone (1.1 ± 0.1 μS) (Fig. 1*E*).

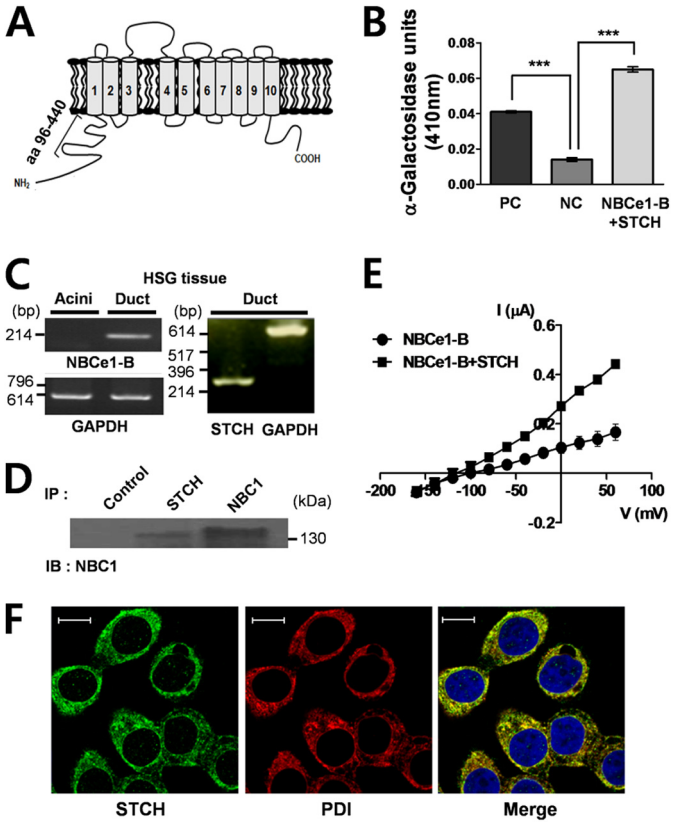

FIGURE 1. **The interaction of NBCe1-B with STCH.** *A*, shown is a schematic diagram of NBCe1-B indicating the position of the bait region (amino acids 96–440) for yeast two-hybrid screening. *B*, shown is an α-galactosidase assay. The positive control (*PC*, $n = 3$) is comprised of the well characterized interaction between p53 (bait) and SV40 large T-antigen (target). The negative control (*NC*) is a co-transformation of human lamin C (bait) and SV40 large T-antigen (target), which is known to have no interaction. ($n = 3$, ***, $p < 0.0001$). NBCe1-B + STCH is a co-transformation of bait region (amino acids 96–440) and STCH (target). ($n = 3$, *** $p < 0.0001$). *C*, NBCe1-B transcripts (*left panel*, $n = 2$) and STCH transcripts (*right panel*, $n = 2$) in primary hSMG ducts are shown. *D*, hSMG tissues were subjected to immunoprecipitation (*IP*) with normal rabbit IgG (*Control*), rabbit anti-STCH, and rabbit anti-NBC1 antibodies. Immunoprecipitates were subjected to Western blotting (*IB*) with rabbit anti-NBC1 antibody ($n = 2$). *E*, shown is the current-voltage (*I-V*) relationship of NBCe1-B current in oocytes injected with cRNA of NBCe1-B or NBCe1-B + STCH. Reversal potentials were −96.54 mV (NBCe1-B, $n = 4$) and −114.4 mV (NBCe1-B +STCH, $n = 6$). *F*, shown is immunolabeling of cultured HSG cell using polyclonal anti-STCH (*green*, *left*, $n = 3$); monoclonal anti-protein disulfide isomerase (*PDI*) antibody (*red*, *middle*, $n = 3$) was used for detection of endoplasmic reticulum. A merged image of double staining is shown on the *right*. *Scale bars*, 10 μm.

TABLE 1

Growth of colonies on selective medium after cotranformation of bait (aa 96–440) and a human submandibular gland library

Selective medium	Number of colonies
−Trp	$>1.0 \times 10^6$
− Leu	$>1.5 \times 10^6$
−Trp/−Leu	>49,000
−Trp/−Leu/−His	441
−Ade/−Trp/−Leu/−His	30

STCH is known to be a microsome-associated chaperone (15). Therefore. we checked for labeling of endogenous STCH in the ER of an HSG cell. Consistent with previous studies, confocal immunofluorescence shows that STCH (*green*) was co-localized with the ER marker, protein disulfide isomerase (*PDI*); *red*) (Fig. 1*F*).

TABLE 2
Proteins interacting with bait (aa 96–440)

Protein	Number of colonies	GenBank™ no.
Immunoglobulin κ constant	1	BC070334
Prokineticin 1	1	AL358215
STCH	5	NM_006948.4

The Essential NBCe1-B Domain for the Functional Interaction with STCH—Having confirmed the interaction between endogenous NBCe1-B and STCH, we next sought to determine the essential binding domains. Two NBCe1-B mutants were constructed in which a portion of the N-terminal domain had been deleted (Δ95aa and Δ345aa) (Fig. 2*A*) and were characterized electrophysiologically using a *Xenopus* oocyte expression system. Oocytes were injected with wild type or mutant NBCe1-B cRNA, and the current-voltage (*I-V*) relationship of the resultant NBCe1-B transporter activity was determined by applying step voltage pulses. The Δ95aa mutant showed ~6-fold increase (6.0 ± 0.2 μS) in conductance compared with wild type of NBCe1-B (1.1 ± 0.1 μS), whereas the Δ345aa mutant showed no detectable transporter activity (Fig. 2*B*). The enhanced activity of the Δ95aa mutant alone compared with wild type suggests that the N-terminal region (aa 1–95) of NBCe1-B includes an essential autoinhibitory domain that regulates the intrinsic activity of NBCe1-B (11).

We next examined the effect of STCH on the activity of NBCe1-B and the Δ95aa mutant in *Xenopus* oocytes by recording the Na^+-dependent change in membrane potential in a HCO_3^--containing solution. Oocytes co-transfected with STCH cRNA displayed ~60% greater membrane hyperpolarization compared with NBCe1-B cRNA alone. Wild type NBCe1-B-mediated hyperpolarization increased from −20.3 ± 1.7 to −33.1 ± 1.9 mV (Fig. 2*C*), and Δ95aa mutant-mediated hyperpolarization increased from −38.7 ± 3.2 to −65.0 ± 4.5 mV (Fig. 2*D*) when co-expressed with STCH. Consistent with the increase in NBCe1-B-mediated current (Fig. 2*B*), Δ95aa mutant showed ~2-fold greater membrane hyperpolarization compared with wild type both in the presence and absence of STCH (Fig. 2, *C* and *D*, *right panels*). These results suggest that STCH enhances NBCe1-B activity via a mechanism distinct from the effect of the Δ95aa mutation.

The Effect of STCH on NBCe1-B Membrane Expression in Xenopus Oocytes—We hypothesized that STCH may enhance NBCe1-B functional activity by increasing its expression. To examine this possibility we performed Western blotting on membrane extracts prepared from cRNA-injected oocytes and analyzed the effect of STCH on the membrane expression of NBCe1-B. Co-expression of STCH in oocytes enhanced the membrane expression of both wild type (Fig. 3*A*, *left panel*) and Δ95aa mutant (Fig. 3*A*, *middle panel*) NBCe1-B compared with NBCe1-B cRNA alone. Densitometry analysis showed that expression of the wild type and Δ95aa mutant was increased approximately 2- and 4-fold, respectively (Fig. 3*B*, *left* and *middle panels*) by STCH co-expression. STCH had no effect on the membrane expression of the non-interacting Δ345aa mutant (Fig. 3, *A* and *B*, *right panel*). STCH also increased the intensity of NBCe1-B immunolabeling near the plasma membrane in oocytes as shown by confocal fluorescence microscopy (Fig. 3, *C* and *D*). These results are consistent with an increase in NBCe1-B protein expression by STCH.

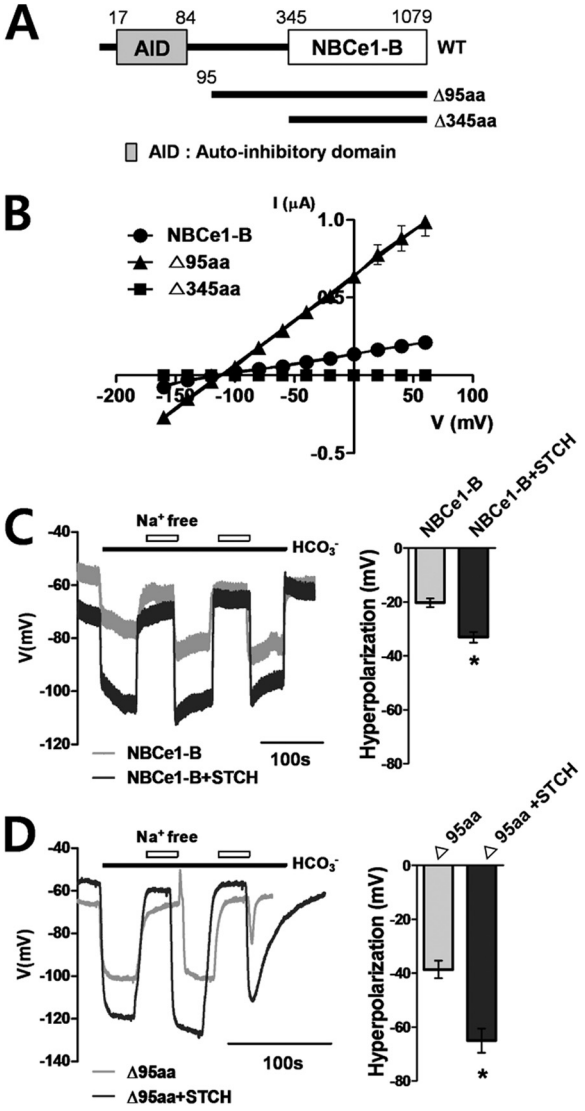

FIGURE 2. **The functional effect of STCH on NBCe1-B activity in *Xenopus* oocytes.** *A*, shown is a diagram of wild type and NBCe1-B deletion mutants. *AID*, autoinhibitory domain. *B*, shown is the current-voltage (*I-V*) relationship of NBCe1-B current in *Xenopus* oocytes injected with cRNA for NBCe1-B wild type, Δ95aa, and Δ345aa. Reversal potentials were −96.54 mV (NBCe1-B, $n = 4$) and −111.9 mV (Δ95aa, $n = 5$). *C* and *D*, shown are membrane potential (V_m) changes by exposure to HCO_3^-/Na^+ or Na^+-free solution mediated by NBCe1-B wild type ($n = 6$) and Δ95aa mutant ($n = 7$) alone or co-expressed with STCH (wild type, $n = 7$; Δ95aa mutant, $n = 9$. *, $p < 0.05$) in oocytes.

Using a co-immunoprecipitation assay we confirmed that truncation of the distal region of NBCe1-B (Δ95aa mutant) did not affect its interaction with STCH. However, larger deletion of the NBCe1-B N-terminal (Δ345aa mutant) completely abrogated the interaction (Fig. 3*E*). These results are in line with the enhancement of functional expression of NBCe1-B and indicate that the region between aa96–345 of NBCe1-B is critical for the interaction with STCH.

Previous studies reported that IRBIT increases the activity of NBCe1-B (9). Therefore, we tested whether STCH may indirectly regulate NBCe1-B by interacting with IRBIT. First, we examined the effect of co-expression of IRBIT with STCH on

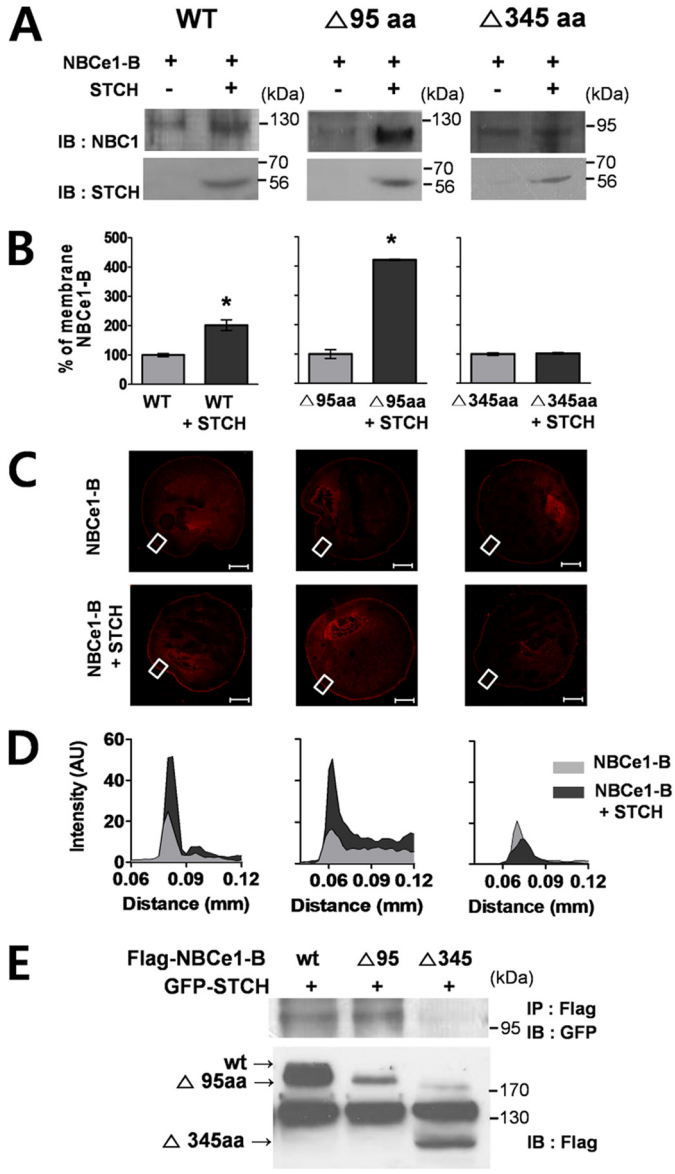

FIGURE 3. **STCH binds to specific regions of NBCe1-B.** *A*, *Xenopus* oocytes ($n = 30$ per transcript) injected with indicated cRNAs were extracted, and membrane fractions were subjected to Western blotting (*IB*) with indicated antibodies. Observations were repeated in at least two independent experiments for each construct: WT ($n = 3$), Δ95aa ($n = 3$), Δ345aa ($n = 2$). *B*, shown is densitometry quantification of bands illustrating wild type and mutant NBCe1 membrane expression in the presence of STCH as a percentage of control (without STCH) (*, $p < 0.05$). *C*, shown is immunolabeling of NBCe1-B wild type and deletion mutants in *Xenopus* oocytes transfected with NBCe1 alone (*upper panels*) or co-transfected with STCH (*lower panels*). *Scale bars*, 200 μm. Images are representative of two to three independent experiments for each transfection. *D*, shown is fluorescence intensity of membrane region corresponding to *white boxed* area in *C*. *AU*, absorbance units. *E*, HSG cells were transfected with FLAG-NBCe1-B, deletion mutants (Δ95aa, Δ345aa), and GFP-STCH plasmid. Cell lysates were subjected to immunoprecipitation (*IP*) with mouse anti-FLAG antibody, and immunoprecipitates were subjected to Western blotting with mouse anti-GFP antibody ($n = 2$).

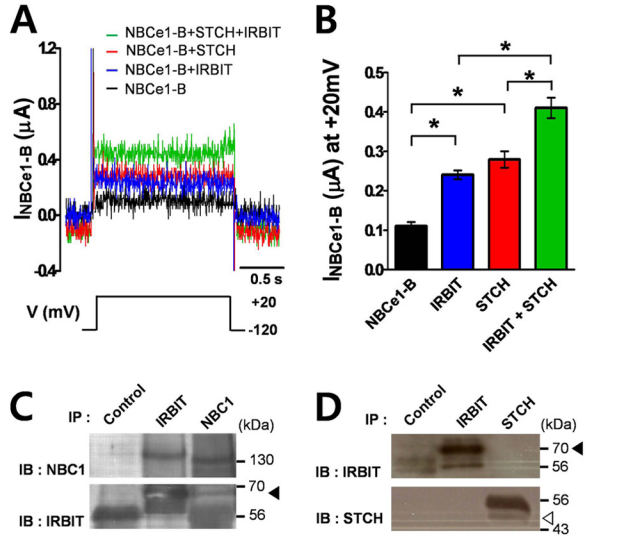

FIGURE 4. **STCH interaction with NBCe1-B occurs independently of IRBIT.** *A*, NBCe1 currents measured in oocytes co-expressed with STCH and/or IRBIT were evoked by a single depolarizing step pulse from −120 to +20 mV in a HCO_3^- solution. *B*, shown is a summary of mean current amplitude at +20 mV in oocytes transfected with NBCe1-B ($n = 5$), IRBIT ($n = 4$; *, $p < 0.05$), and STCH ($n = 6$; *, $p < 0.05$) either alone or as co-transfection ($n = 4$; *, $p < 0.05$). *C*, HSG cells were subjected to immunoprecipitation (*IP*) with normal mouse IgG, mouse anti-IRBIT, and anti-NBC1 antibodies. Immunoprecipitates were subjected to Western blotting (*IB*) with anti-NBC1 ($n = 2$) and anti-IRBIT ($n = 2$) antibodies. The *filled triangle* indicates the migration of endogenous IRBIT. *D*, HSG cells were subjected to immunoprecipitation with anti-STCH and anti-IRBIT antibodies. Immunoprecipitates were subjected to Western blotting with anti-STCH ($n = 2$) and anti-IRBIT ($n = 2$) antibodies. *Filled* and *empty triangles* indicate the migration of endogenous IRBIT and STCH, respectively.

the activity of NBCe1-B in *Xenopus* oocyte by measuring NBCe1-B-mediated current in response to a depolarizing step from −120 to +20 mV. Injection of IRBIT cRNA increased NBCe1-B currents in *Xenopus* oocytes by 116% (0.24 ± 0.01 μA), whereas injection of STCH cRNA increased NBCe1-B current by 151% (0.28 ± 0.02 μA) compared with NBCe1-B cRNA alone (0.11 ± 0.01 μA) (Fig. 4*A*). However, co-injection of IRBIT and STCH cRNA together with NBCe1-B resulted in a cumulative enhancement of NBCe1-B current by 299% (0.41 ± 0.03 μA) (Fig. 4*B*). Although we confirmed the interaction of IRBIT with NBCe1-B (Fig. 4*C*), STCH did not co-immunoprecipitate with IRBIT in HSG cells (Fig. 4*D*), suggesting that there is no cross-interaction between STCH and IRBIT in the regulation of NBCe1-B activity.

Role of Endogenous STCH in HSG Cells—To investigate the effect of endogenous STCH on the function of NBCe1-B, we silenced endogenous STCH expression by RNA interference in HSG cells. Endogenous expression of NBCe1-B and STCH, but not the NBCe1-A isoform, was confirmed using RT-PCR (Fig. 5*A*). The list of DNA primer sequences is shown in Table 3. Two independent siRNA constructs were tested (Table 4); siRNA sequences 1 and 2 reduced STCH expression by ~80 and ~60%, respectively (Fig. 5, *B* and *C*). siRNA1 was used for further experiments.

Next, we examined the functional effect of STCH siRNA knockdown on Na^+-dependent pH_i recovery from NH_4^+ pulse in HSG cells. The pH fluorescence ratio of BCECF-AM-loaded HSG cells was measured in a bath solution containing Na^+ and HCO_3^- ions (see "Experimental Procedures"). The antagonists DIDS and EIPA were used to block the activity of endogenous NBCe1-B and NHE, respectively. pH_i recovery in the presence of control scrambled siRNA revealed an EIPA- and DIDS-sensitive component, suggesting that both NHE and NBCe1-B contribute to normal pH_i recovery in HSG cells. Silencing of STCH by specific siRNA decreased the overall rate of pH_i recovery by ~72% (0.024 ± 0.003) compared with scrambled

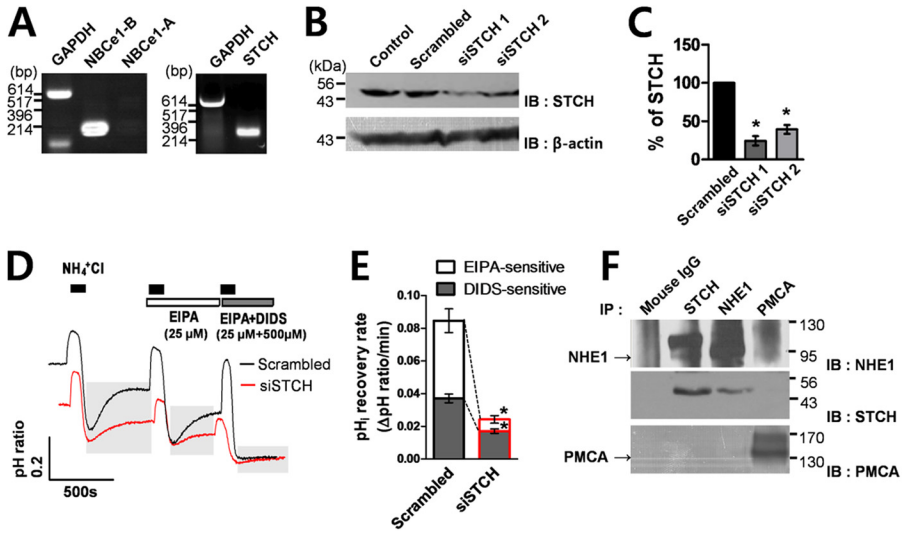

FIGURE 5. **Knockdown of STCH inhibits pH_i recovery from acidification.** *A*, shown are NBCe1-B (*left panel*, $n = 2$) and STCH transcripts (*right panel*, $n = 2$) in HSG cells. Note PCR products for NBCe1-A were not observed (*left panel*). *B*, HSG cells were transfected with one of two siRNA sequences targeting STCH or scrambled siRNA. *IB*, immunoblot. *C*, densitometry quantification of bands illustrating STCH expression in the presence of STCH siRNA 1 ($n = 3$) and 2 ($n = 3$) as a percentage of control (scrambled siRNA) ($n = 3$; *, $p < 0.05$). *D*, Na^+-dependent pH_i recovery from NH_4^+ pulse (*black bars*) in HSG cells in the presence of STCH (the resting pH_i of cells was ~6.92, $n = 5$; *, $p < 0.05$) or scrambled siRNA (the resting pH_i of cells was ~7.45, $n = 5$) recorded in a HCO_3^- solution. EIPA (25 μM) and DIDS (500 μM) applications are indicated by the *horizontal bars*. *E*, shown is a summary quantification of the EIPA ($n = 5$; *, $p < 0.05$)- and DIDS-sensitive ($n = 5$; *, $p < 0.05$) pH_i recovery rate in the presence of scrambled or STCH siRNA. *F*, HSG cells were subjected to immunoprecipitation with mouse IgG, anti-STCH, anti-NHE1, and mouse anti-PMCA antibodies. Immunoprecipitates (*IP*) were subjected to Western blotting (*IB*) with anti-NHE1 ($n = 2$), anti-STCH ($n = 2$), and anti-PMCA ($n = 2$) antibodies. In the case of Western blotting with anti-STCH (*second panel*), ReliaBLOT reagents were used to remove contaminating heavy chain IgG (see "Experimental Procedures").

TABLE 3
List of DNA primers sequences designed for reverse transcription PCR

Target gene	Length	Forward primers	Reverse primers	GenBank™ no.
	bp			
NBCe1-B	246	5′-gct tcc ttc ctc aag cat gt-3′	5′-tag gat gct gct gct gga tt-3′	AF_011390.1
NBCe1-A	982	5′-act ttc ctc agg gtt gtc cag-3′	5′-agc atg aca gcc tgc tgt a-3′	NM_003759.3
STCH	270	5′-atg gca gag gca tat ctt gg-3′	5′-tgc tcg ggt tag aaa cat cc-3′	NM_006948.4
GAPDH	605	5′-gga agg tga agg tcg gag tc-3′	5′-cag tag agg cag gga tga tg-3′	M_33197

TABLE 4
List of siRNA sequences designed for silencing STCH

Target gene	siRNA sequence
STCH	5′-GGG CAU AAC AGC AUU CCA ATT-3′
siRNA1	5′-UUG GAA UGC UGU UAU GCC CTT-3′
STCH	5′-GCA AAU CCU CAG AAC ACU ATT-3′
siRNA2	5′-UAG UGU UCU GAG GAU UUG CTT-3′
Scrambled	5′-UUC UCC GAA CGU GUC ACG UTT-3′
siRNA	5′-ACG UGA CAC GUU CGG AGA ATT-3′

siRNA (0.085 ± 0.006) (Fig. 5*D*). Quantification of the pH_i recovery rate in the presence and absence of each antagonist revealed that STCH siRNA decreased the pH_i recovery rate of the DIDS-sensitive component by ~54% (0.017 ± 0.001) and EIPA-sensitive component by ~85% (0.007 ± 0.002) compared with control (Fig. 5*E*). These data suggest that STCH siRNA significantly reduced both NBCe1-B and NHE-mediated pH_i recovery, respectively. NHE1 is the major ion exchanger subtype known to be expressed in the basolateral membrane of hSMG duct cells (22). We confirmed that endogenous STCH interacted with NHE1 in HSG cells using co-immunoprecipitation (Fig. 5*F*). PMCA is also found in submandibular glands where it plays a vital role in regulating intracellular Ca^{2+} (23). However, no interaction was observed between STCH and the PMCA (Fig. 5*F*).

To definitively test whether STCH modulates the functional expression of NBCe1-B at the plasma membrane specifically, we performed an additional surface biotinylation assay. Consistent with Western blot data from whole membrane fractions (Fig. 3*A*), STCH significantly increased the level of surface biotinylated NBCe1-B (Fig. 6, *A* and *B*). Conversely, detection of biotinylated NBCe1-B was decreased by STCH siRNA (Fig. 6, *D* and *E*). Plasma membrane expression of PMCA, serving as a negative control, remained unchanged in both experiments (Fig. 6, *C* and *F*).

The Effect of STCH on NHE-mediated pH_i Regulation in HSG Cells—To confirm the specificity of the effect of STCH on the functional activity of NHE in HSG cells, we recorded Na^+-dependent, EIPA-sensitive pH_i recovery from NH_4^+ pulse in a HEPES-buffered (HCO_3^--free) solution. Overexpression of STCH in HSG cells increased pH_i recovery rate by ~150% (0.025 ± 0.002) compared with empty vector (0.010 ± 0.002) (Fig. 7, *A* and *B*) and increased surface membrane expression of NHE1 by ~128% in a biotinylation assay (Fig. 7, *C* and *D*). Conversely, transfection of STCH siRNA reduced the EIPA- sensitive pH_i recovery rate by ~56% (0.004 ± 0.001) compared with scrambled siRNA (0.009 ± 0.001) (Fig. 7, *E* and *F*). Surface biotinylation analysis shows that STCH siRNA reduced expression of NHE1 at the cell surface by ~50% (Fig. 7, *G* and *H*). Together these results suggest that endogenous STCH dynamically regulates NHE activity and surface expression.

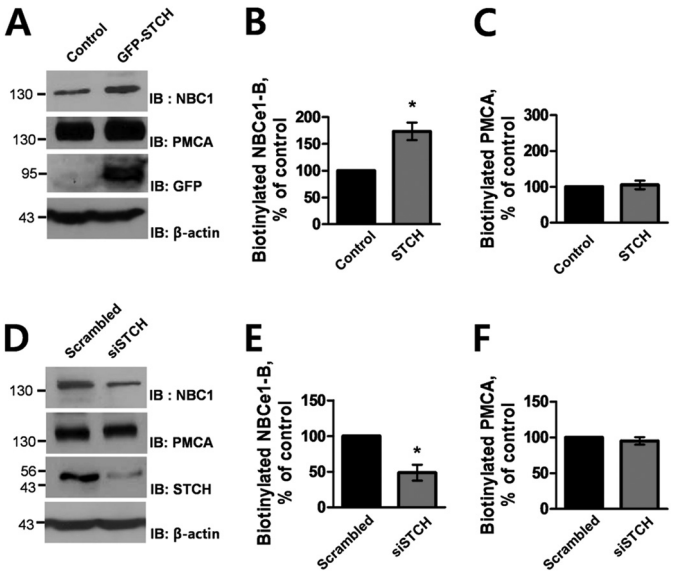

FIGURE 6. **Effect of STCH on surface expression of NBCe1-B.** *A*, HSG cells were transfected with empty vector or STCH. Surface-biotinylated proteins (1 mg) were subjected to Western blotting (*IB*) with rabbit anti-NBC1 and anti-PMCA, and whole cell lysates were subjected to Western blotting with anti-GFP and anti-β-actin antibodies. Densitometry quantification of bands illustrate NBCe1-B surface expression ($n = 3$; *, $p < 0.05$; *B*) and PMCA surface expression ($n = 3$; *C*) in the presence of STCH as a percentage of control (without STCH). *D*, HSG cells were transfected with scrambled or STCH siRNA. Surface-biotinylated proteins (1 mg) were subjected to Western blotting with rabbit anti-NBC1 and anti-PMCA, and whole cell lysates were subjected to Western blotting with anti-STCH and anti-β-actin antibodies. Densitometry quantification of bands illustrating NBCe1 surface expression ($n = 3$; *, $p < 0.05$; *E*) and PMCA surface expression ($n = 3$; *F*) in the presence of STCH siRNA as a percentage of control (scrambled siRNA).

Essential STCH Domain for Transporter Interaction—As shown in Fig. 8*A*, STCH has five consensus ATP binding domains that are conserved throughout the Hsp70 family (24) as well as three STCH-specific clusters that are homologous between rat and human species (25). However, STCH also possesses a unique 45-amino acid C-terminal domain (aa 314–358) that is not found in other ER chaperones (25). To examine the essential STCH binding domain(s) and to confirm the specificity of the interaction with NBCe1-B and NHE1, we generated two deletion mutants of STCH, Δ314aa and Δ359aa, that lacked the unique 45-amino acid region of STCH (Fig. 8*A*). Wild type and Δ314 STCH both co-immunoprecipitated with wild type NBCe1-B, but no apparent interaction was observed with the Δ359 STCH mutant (Fig. 8*B*). A similar result was obtained when the STCH variants were co-immunoprecipitated with wild type NHE1 (Fig. 8*C*). Each blot was repeated three times. In summary, both NBCe1-B and NHE1 interactions were dependent on aa314–358 in STCH (Fig. 8, *B* and *C*; thus our study is the first to report a role for this unique region (aa 314–358) through an interaction with membrane transporters.

DISCUSSION

In this study we used yeast-two hybrid screening to identify novel interacting partners of NBCe1-B in HSG cells. We identified STCH, a microsome-associated stress 70 protein, as a candidate NBCe1-B and NHE1 binding molecule.

STCH Regulation of NBCe1—We initially focused our efforts on elucidating the biological function of STCH in regulating NBCe1-B activity. Co-injection of STCH cRNA in *Xenopus* oocytes resulted in stimulation of NBCe1-B transport activity via trafficking to the plasma membrane. Moreover, silencing of endogenously expressed STCH interfered with pH_i regulation by inhibiting DIDS-sensitive pH_i recovery in HSG cells. These results suggest that endogenous STCH expression is necessary for full NBCe1-B activity and normal rate of pH_i recovery in HSG cells. We also demonstrated that STCH maintains an interaction with the Δ95aa mutant of NBCe1-B. In an electrophysiological study we observed that STCH enhanced the activity of Δ95aa NBCe1-B mutant and increased its surface expression in *Xenopus* oocytes. By confirming the lack of interaction between STCH and Δ345aa NBCe1-B mutant, we can conclude that aa96–345 region of NBCe1-B is critical for the physical and functional interaction with STCH and highlights the importance of the NBCe1-B N terminus for targeting to the plasma membrane. Based on the sequence homology of this region between members of the NBC1 transporter family, we speculate that STCH may also interact with the kidney type NBCe1, NBCe1-A as well as electroneutral NBCn1 (electroneutral Na^+/HCO_3^- co-transporter 1).

As the most well known mechanism of NBCe1-B regulation there remained the possibility that IRBIT was involved in the STCH-mediated modulation of NBCe1-B expression. However, STCH did not interact with IRBIT, and no cross-interaction between STCH and IRBIT was observed on the regulation of NBCe1-B transport activity in *Xenopus* oocytes, suggesting that STCH represents a novel regulatory molecule associated with NBCe1-B activity.

STCH Regulation of NHE1—In the course of our functional analysis of STCH in pH_i regulation we uncovered a further interaction between STCH and NHE1. Na^+/H^+ exchange plays an important role in pH_i recovery in submandibular gland (5). A previous study in human submandibular duct cells reported that NHE1 and NHE3 subtypes are expressed at the basolateral and apical membranes, respectively (22). In HCO_3^--buffered solution, intracellular acidification induces the activity of NHE and NBCe1-B to recover pH_i in a Na^+-dependent manner. Under these conditions we show that both NHE and NBCe1-B contribute to pH_i regulation in HSG cells by measuring the pH_i recovery component blocked by the selective transporter antagonists EIPA and DIDS, respectively. Surprisingly we observed that knockdown of STCH with siRNA decreased both the EIPA- and DIDS-sensitive components of Na^+-dependent pH_i recovery compared with control, suggesting a functional interaction with NHE transportation. We further show that NHE-mediated pH_i recovery is sensitive to STCH siRNA and that overexpression of STCH in HSG cells increased NHE1-dependent pH_i recovery. Using co-immunoprecipitation analysis we confirmed a direct interaction between endogenous STCH and NHE1. Together these results suggest that endogenous STCH dynamically regulates NHE1 activity.

The plasma membrane Ca^{2+} ATPase, PMCA, is another ion transporter that affects intracellular pH by exchanging intracellular Ca^{2+} for extracellular H^+. Our laboratory has previously reported an endogenous mechanism of intracellular acidification that is mediated by PMCA, which involves a rise in intracellular Ca^{2+} induced by glutamate or capsaicin in sensory neu-

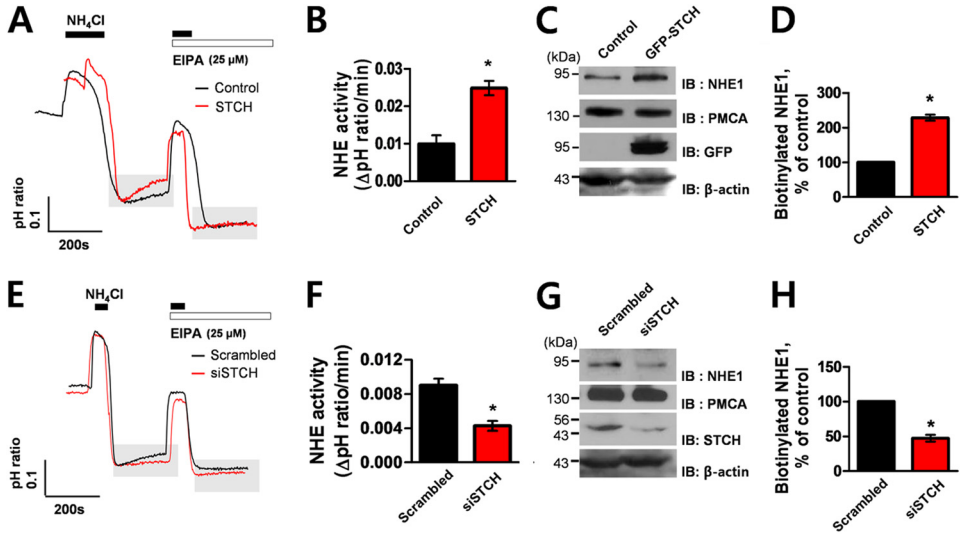

FIGURE 7. **Effect of STCH on the functional activity of NHE.** *A*, shown is Na^+-dependent pH_i recovery from NH_4^+ pulse (*black bars*) in HSG cells transfected with STCH (the resting pH_i of cells was ~7. 63) or empty vector (the resting pH_i of cells was ~7.40, control) in a HCO_3^--free solution and the effect of EIPA (25 μM) application (*white bar*). *B*, summary quantification of the EIPA-sensitive pH_i recovery rate with ($n = 4$; *, $p < 0.05$) or without STCH ($n = 3$) transfection is shown. *C*, HSG cells were transfected with empty vector or STCH. Surface-biotinylated proteins (1 mg) were subjected to Western blotting with rabbit anti-NHE1 and anti-PMCA, and whole cell lysates were subjected to Western blotting (*IB*) with anti-GFP and anti-β-actin antibodies. *D*, densitometry quantification of bands illustrating NHE1 surface expression ($n = 3$; *, $p < 0.05$) is shown in the presence of STCH as a percentage of control (without STCH). *E*, shown is Na^+-dependent pH_i recovery from NH_4^+ pulse (*black bars*) in HSG cells in the presence of STCH (the resting pH_i of cells was ~7.11) or scrambled siRNA (the resting pH_i of cells was ~7.10) recorded in a HCO_3^--free solution and the effect of EIPA (25 μM) application (*white bar*). *F*, shown is summary quantification of the EIPA-sensitive pH_i recovery rate in the presence of scrambled ($n = 5$) or STCH siRNA ($n = 5$; *, $p < 0.05$). *G*, HSG cells were transfected with scrambled or STCH siRNA. Surface-biotinylated proteins (1 mg) were subjected to Western blotting with rabbit anti-NHE1 and anti-PMCA, and whole cell lysates were subjected to Western blotting with anti-STCH and anti-β-actin antibodies. *H*, shown is densitometry quantification of bands illustrating NHE1 surface expression ($n = 3$; *, $p < 0.05$) in the presence of STCH siRNA as a percentage of control (scrambled siRNA).

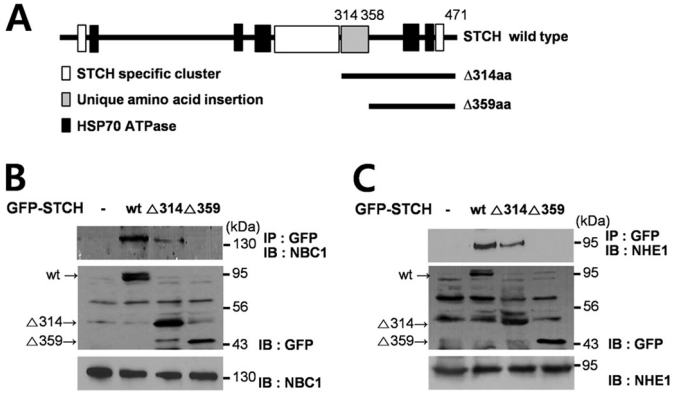

FIGURE 8. **Specific region of STCH required for interaction with NBCe1-B and NHE1.** *A*, shown are diagrams of wild type STCH and two STCH deletion mutants. *B* and *C*, HSG cells were transfected with GFP-tagged wild type, Δ314aa, and Δ359aa STCH. Cell lysates were subjected to immunoprecipitation with anti-GFP antibody, and immunoprecipitates (*IP*) were subjected to Western blotting (*IB*) with anti-NBC1 ($n = 3$) (*B*) or anti-NHE1 antibodies ($n = 3$) (*C*) (*upper panels*). To confirm transfection efficiency of GFP-tagged constructs, whole lysates of HSG cells were subjected to Western blotting with anti-GFP (*middle panels*). Endogenous expression of NBC1 and NHE1 was confirmed with anti-NBC1 and anti-NHE1 antibodies, respectively (*lower panels*).

rons (26). However, we observed no interaction between STCH and the acidifying transporter PMCA. This result is in keeping with the functional enhancement ion transporters specifically involved in the recovery from acidification. Therefore, we speculate that STCH interactions may generally function to affect the activity of membrane transporters that operate to raise pH_i in response to disruption of ionic homeostasis. The wide expression STCH in human tissues (15) suggests a conserved mechanism of pH_i regulation; our results obtained in epithelial cells further suggest a potential role of STCH in modulation of fluid secretion from glandular tissues through its effect on HCO_3^- transportation.

Role of STCH as an ER Chaperone—Structurally STCH possesses a unique 45-amino acid C-terminal domain (aa 314–358) as well as other insertions and clusters specific to STCH (25). Our study is the first to report a role for this unique region through an interaction with membrane transporters. Both NBCe1-B and NHE1 interactions were dependent on aa 314–359 in STCH. Together our results suggest a significant role for STCH, specifically the aa 314–359 region, in pH_i regulation.

There are two previous reports of NHE1 interacting with heat shock protein 70 (27, 28). Although Hsp70 does not include the same region of STCH (aa 314–359), it does possess several partner proteins with which it functions in the cell. For example Hsp70 interacting protein (Hip) is proposed to function as a co-chaperone by directly binding to the N-terminal domain of Hsp70 (29). Interestingly, there are sequence similarities between STCH (aa 261–296) and a 34-amino acid region of the Hip protein (29), which is required for direct binding of Hip to the Hsp70 ATPase domain. Therefore, we hypothesize that STCH might play a role in protein synthesis by acting as a co-chaperone with Hsp70.

STCH was localized in the ER compartment and exerted its effect on pH_i by regulating the functional expression of both NHE1 and NBCe1-B. This new description of STCH function may be compared with another Hsp70 family member, Bip, that regulates the surface expression of ligand-gated ion channels (30). Bip protein possesses a 36-amino acid region that shares similarities with a 35-amino acid domain (aa 411–445) of STCH (21). Bip also plays a variety of roles in the ER, including the translocation of newly synthesized proteins across the ER

membrane (31, 32). The ER contains a number of protein chaperones that are involved in post-translational modification, folding, assembly, and quality control of newly synthesized proteins. Furthermore, up-regulation of ER chaperones is essential to preserve cellular homeostasis at times of cellular stress such as changes to pH_i. Therefore, it is tempting to speculate that STCH, like Bip, may be involved in the quality control of newly synthesized transporters by functioning as an ER chaperone. It remains to be investigated whether STCH levels in the ER are up-regulated in response to homeostatic stressors.

STCH-related Pathologies—Recent studies have reported that STCH is a candidate gene involved in certain cancers (20, 33, 34) as well as several central nervous system pathologies (16–18). Our new description of the STCH chaperone as a pH_i regulator points to several potential consequences of its malfunction that may shed light on these reports. For example, during energy deficiency a loss-of-function of STCH may result in a failure to up-regulate NBCe1 within neurons; the subsequent lack of acid extrusion could feasibly contribute to the well recognized intracellular acidosis associated with neuronal pathologies (35, 36).

Up-regulation of NHE1 expression and an increase in its functional activity are crucial in cell differentiation (37, 38). Interestingly, the facilitation of cell migration and invasion of cancer cells has been described as a result of a pH gradient switch due to NHE1 overactivity and extracellular acidification (39). In addition, dynamic changes in NHE1 expression have been shown to induce cancer cell death. Thus a new strategy in the development of novel cancer-specific therapeutics is a focus on the disregulation of pH_i (40, 41). Our finding that STCH dynamically regulates NHE1 activity may provide a clue to the reports linking STCH with cancer development.

Conclusion—Our study is the first report of a hitherto unknown role of STCH in the regulation of membrane ion transporter expression and pH_i regulation in secretory epithelial cells via protein-protein interaction. We suggest that STCH may function to enhance recovery from intracellular acidification by increasing the functional expression of NBCe1-B and NHE1 transporters at the cell membrane. Further work will focus on how STCH binding to membrane transporters enhances membrane expression and the molecular mechanisms of this interaction.

REFERENCES

1. Park, K., Hurley, P. T., Roussa, E., Cooper, G. J., Smith, C. P., Thévenod, F., Steward, M. C., and Case, R. M. (2002) Expression of a sodium bicarbonate cotransporter in human parotid salivary glands. *Arch. Oral Biol.* **47,** 1–9
2. Lee, M. G., Ohana, E., Park, H. W., Yang, D., and Muallem, S. (2012) Molecular mechanism of pancreatic and salivary gland fluid and HCO_3 secretion. *Physiol. Rev.* **92,** 39–74
3. Kim, Y. B., Yang, B. H., Piao, Z. G., Oh, S. B., Kim, J. S., and Park, K. (2003) Expression of Na^+/HCO_3^- cotransporter and its role in pH regulation in mouse parotid acinar cells. *Biochem. Biophys. Res. Commun.* **304,** 593–598
4. Li, J., Koo, N. Y., Cho, I. H., Kwon, T. H., Choi, S. Y., Lee, S. J., Oh, S. B., Kim, J. S., and Park, K. (2006) Expression of the Na^+-HCO_3^- cotransporter and its role in pH_i regulation in guinea pig salivary glands. *Am. J. Physiol. Gastrointest Liver Physiol.* **291,** G1031–G1040
5. Choi, S. Y., Li, J., Jo, S. H., Lee, S. J., Oh, S. B., Kim, J. S., Lee, J. H., and Park, K. (2006) Desipramine inhibits Na^+/H^+ exchanger in human submandibular cells. *J. Dent. Res.* **85,** 839–843
6. Kemp, G., Young, H., and Fliegel, L. (2008) Structure and function of the human Na^+/H^+ exchanger isoform 1. *Channels* **2,** 329–336
7. Putney, L. K., and Barber, D. L. (2003) Na-H exchange-dependent increase in intracellular pH times G_2/M entry and transition. *J. Biol. Chem.* **278,** 44645–44649
8. Reshkin, S. J., Bellizzi, A., Caldeira, S., Albarani, V., Malanchi, I., Poignee, M., Alunni-Fabbroni, M., Casavola, V., and Tommasino, M. (2000) Na^+/H^+ exchanger-dependent intracellular alkalinization is an early event in malignant transformation and plays an essential role in the development of subsequent transformation-associated phenotypes. *FASEB J.* **14,** 2185–2197
9. Shirakabe, K., Priori, G., Yamada, H., Ando, H., Horita, S., Fujita, T., Fujimoto, I., Mizutani, A., Seki, G., and Mikoshiba, K. (2006) IRBIT, an inositol 1,4,5-trisphosphate receptor-binding protein, specifically binds to and activates pancreas-type Na^+/HCO_3^- cotransporter 1 (pNBC1). *Proc. Natl. Acad. Sci. U.S.A.* **103,** 9542–9547
10. Yang, D., Li, Q., So, I., Huang, C. L., Ando, H., Mizutani, A., Seki, G., Mikoshiba, K., Thomas, P. J., and Muallem, S. (2011) IRBIT governs epithelial secretion in mice by antagonizing the WNK/SPAK kinase pathway. *J. Clin. Invest.* **121,** 956–965
11. Lee, S. K., Boron, W. F., and Parker, M. D. (2012) Relief of autoinhibition of the electrogenic Na-HCO cotransporter NBCe1-B. Role of IRBIT *vs.* amino-terminal truncation. *Am. J. Physiol. Cell Physiol.* **302,** C518–C526
12. He, P., Zhang, H., and Yun, C. C. (2008) IRBIT, inositol 1,4,5-triphosphate (IP_3) receptor-binding protein released with IP_3, binds Na^+/H^+ exchanger NHE3, and activates NHE3 activity in response to calcium. *J. Biol. Chem.* **283,** 33544–33553
13. Boedtkjer, E., Bunch, L., and Pedersen, S. F. (2012) Physiology, pharmacology, and pathophysiology of the pH regulatory transport proteins NHE1 and NBCn1. Similarities, differences, and implications for cancer therapy. *Curr. Pharm. Des.* **18,** 1345–1371
14. Matsushita, M., Tanaka, H., Mitsui, K., and Kanazawa, H. (2011) Dual functional significance of calcineurin homologous protein 1 binding to Na^+/H^+ exchanger isoform 1. *Am. J. Physiol. Cell Physiol.* **301,** C280–C288
15. Otterson, G. A., Flynn, G. C., Kratzke, R. A., Coxon, A., Johnston, P. G., and Kaye, F. J. (1994) Stch encodes the ATPase core of a microsomal stress 70 protein. *EMBO J.* **13,** 1216–1225
16. Han, P., Wang, X. F., and Wang, L. (2011) Adenosine triphosphate binding gene messenger ribonucleic acid expression in brains of drug-resistant epileptics. *Zhonghua Yi Xue Za Zhi* **91,** 2314–2318
17. Iurov, IIu, Vorsanova, S. G., Saprina, E. A., and Iurov, IuB (2010) Identification of candidate genes of autism on the basis of molecular cytogenetic and *in silico* studies of the genome organization of chromosomal regions involved in unbalanced rearrangements. *Genetika* **46,** 1348–1351
18. Groet, J., Ives, J. H., South, A. P., Baptista, P. R., Jones, T. A., Yaspo, M. L., Lehrach, H., Potier, M. C., Van Broeckhoven, C., and Nizeti, D. (1998) Bacterial contig map of the 21q11 region associated with Alzheimer's disease and abnormal myelopoiesis in Down syndrome. *Genome Res.* **8,** 385–398
19. Heimel, J. A., Hermans, J. M., Sommeijer, J. P., Neuro-Bsik Mouse Phenomics consortium, and Levelt, C. N. (2008) Genetic control of experience-dependent plasticity in the visual cortex. *Genes Brain Behav.* **7,** 915–923
20. Yamagata, N., Furuno, K., Sonoda, M., Sugimura, H., and Yamamoto, K. (2008) Stomach cancer-derived del223V-226L mutation of the STCH gene causes loss of sensitization to TRAIL-mediated apoptosis. *Biochem. Biophys. Res. Commun.* **376,** 499–503
21. Kaye, F. J., Modi, S., Ivanovska, I., Koonin, E. V., Thress, K., Kubo, A., Kornbluth, S., and Rose, M. D. (2000) A family of ubiquitin-like proteins binds the ATPase domain of Hsp70-like Stch. *FEBS Lett.* **467,** 348–355
22. Roussa, E. (2001) H^+ and HCO_3^- transporters in human salivary ducts. An immunohistochemical study. *Histochem. J.* **33,** 337–344
23. Homann, V., Kinne-Saffran, E., Arnold, W. H., Gaengler, P., and Kinne, R. K. (2006) Calcium transport in human salivary glands. A proposed model of calcium secretion into saliva. *Histochem. Cell Biol.* **125,** 583–591
24. Bork, P., Sander, C., and Valencia, A. (1992) An ATPase domain common

to prokaryotic cell cycle proteins, sugar kinases, actin, and hsp70 heat shock proteins. *Proc. Natl. Acad. Sci. U.S.A.* **89,** 7290–7294
25. Otterson, G. A., and Kaye, F. J. (1997) A core ATPase, Hsp70-like structure is conserved in human, rat, and *C. elegans* STCH proteins. *Gene* **199,** 287–292
26. Hwang, S. M., Koo, N. Y., Jin, M., Davies, A. J., Chun, G. S., Choi, S. Y., Kim, J. S., and Park, K. (2011) Intracellular acidification is associated with changes in free cytosolic calcium and inhibition of action potentials in rat trigeminal ganglion. *J. Biol. Chem.* **286,** 1719–1729
27. Xue, J., Zhou, D., Yao, H., Gavrialov, O., McConnell, M. J., Gelb, B. D., and Haddad, G. G. (2007) Novel functional interaction between Na^+/H^+ exchanger 1 and tyrosine phosphatase SHP-2. *Am. J. Physiol. Regul. Integr. Comp. Physiol.* **292,** R2406–R2416
28. Silva, N. L., Haworth, R. S., Singh, D., and Fliegel, L. (1995) The carboxyl-terminal region of the Na^+/H^+ exchanger interacts with mammalian heat shock protein. *Biochemistry* **34,** 10412–10420
29. Höhfeld, J., Minami, Y., and Hartl, F. U. (1995) Hip, a novel cochaperone involved in the eukaryotic Hsc70/Hsp40 reaction cycle. *Cell* **83,** 589–598
30. Wanamaker, C. P., and Green, W. N. (2007) Endoplasmic reticulum chaperones stabilize nicotinic receptor subunits and regulate receptor assembly. *J. Biol. Chem.* **282,** 31113–31123
31. Corsi, A. K., and Schekman, R. (1997) The lumenal domain of Sec63p stimulates the ATPase activity of BiP and mediates BiP recruitment to the translocon in *Saccharomyces cerevisiae*. *J. Cell Biol.* **137,** 1483–1493
32. McClellan, A. J., Endres, J. B., Vogel, J. P., Palazzi, D., Rose, M. D., and Brodsky, J. L. (1998) Specific molecular chaperone interactions and an ATP-dependent conformational change are required during posttranslational protein translocation into the yeast ER. *Mol. Biol. Cell* **9,** 3533–3545
33. Aoki, M., Yamamoto, K., Ohyama, S., Yamamura, Y., Takenoshita, S., Sugano, K., Minamoto, T., Kitajima, M., Sugimura, H., Shimada, S., Noshiro, H., Hiratsuka, M., Sairenji, M., Ninomiya, I., Yano, M., Uesaka, K., Matsuno, S., Maehara, Y., Aikou, T., and Sasazuki, T. (2005) A genetic variant in the gene encoding the stress70 protein chaperone family member STCH is associated with gastric cancer in the Japanese population. *Biochem. Biophys. Res. Commun.* **335,** 566–574
34. Worsham, M. J., Lu, M., Chen, K. M., Stephen, J. K., Havard, S., and Schweitzer, V. P. (2012) Malignant and nonmalignant gene signatures in squamous head and neck cancer. *J. Oncol.* **2012,** 752860
35. Yao, H., and Haddad, G. G. (2004) Calcium and pH homeostasis in neurons during hypoxia and ischemia. *Cell Calcium* **36,** 247–255
36. Tombaugh, G. C., and Sapolsky, R. M. (1993) Evolving concepts about the role of acidosis in ischemic neuropathology. *J. Neurochem.* **61,** 793–803
37. Rao, G. N., Sardet, C., Pouysségur, J., and Berk, B. C. (1993) Phosphorylation of Na^+-H^+ antiporter is not stimulated by phorbol ester and acidification in granulocytic HL-60 cells. *Am. J. Physiol.* **264,** C1278–C1284
38. Dyck, J. R., Maddaford, T. G., Pierce, G. N., and Fliegel, L. (1995) Induction of expression of the sodium-hydrogen exchanger in rat myocardium. *Cardiovasc. Res.* **29,** 203–208
39. Loo, S. Y., Chang, M. K., Chua, C. S., Kumar, A. P., Pervaiz, S., and Clement, M. V. (2012) NHE-1. A promising target for novel anti-cancer therapeutics. *Curr. Pharm. Des.* **18,** 1372–1382
40. Neri, D., and Supuran, C. T. (2011) Interfering with pH regulation in tumours as a therapeutic strategy. *Nat. Rev. Drug Discov.* **10,** 767–777
41. Webb, B. A., Chimenti, M., Jacobson, M. P., and Barber, D. L. (2011) Dysregulated pH. A perfect storm for cancer progression. *Nat. Rev. Cancer* **11,** 671–677